Intrinsic and tumor-induced JAK/STAT signaling regulate developmental timing by the *Drosophila* prothoracic gland

Xueya Cao[1] and José Carlos Pastor-Pareja[1,2*]

[1] School of Life Sciences, Tsinghua University, Beijing, China

[2] Tsinghua-Peking Center for Life Sciences, Beijing, China

* Correspondence: josepastor@tsinghua.edu.cn

Contact:

José Carlos Pastor-Pareja

School of Life Sciences, Tsinghua University

Medical Science Bldg., D224

Beijing 100084, China

Tel: (+86) 10-627-83498

http://joselab.life.tsinghua.edu.cn

ORCID: 0000-0002-3823-4473

Abstract

Development involves tightly paced, reproducible sequences of events, yet it must adjust to conditions external to it, such as resource availability and organismal damage. A major mediator of damage-induced immune responses in vertebrates and insects is JAK/STAT signaling. At the same time, JAK/STAT activation by the *Drosophila* Upd cytokines is pleiotropically involved in normal development of multiple organs. Whether inflammatory and developmental roles of JAK/STAT intersect is unknown. Here, we show that JAK/STAT is active during development of the prothoracic gland (PG), the organ that controls metamorphosis onset through ecdysone production. Reducing JAK/STAT signaling decreased PG size and slightly advanced metamorphosis. Conversely, JAK/STAT hyperactivation, achieved through overexpression of pathway components or SUMOylation loss, caused PG hypertrophy and metamorphosis delay. Interestingly, tissue damage and tumors, known to secrete Upd cytokines, also activated JAK/STAT in the PG and delayed metamorphosis. Finally, we show that expression of transcription factor Apontic, a JAK/STAT target in the PG, recapitulates PG hypertrophy and metamorphosis delay. JAK/STAT damage signaling, therefore, regulates metamorphosis onset at least in part by coopting its developmental role in the PG.

Keywords:

Metamorphosis, ring gland, ecdysone, tissue damage, inflammation, SUMOylation

Summary statement:

Damage signaling from tumors mediated by JAK/STAT-activating Upd cytokines delays the *Drosophila* larva-pupa transition through cooption of a JAK/STAT developmental role in the prothoracic gland.

43 **INTRODUCTION**

44 The development of organisms involves internally paced, reproducible sequences of molecular
45 and cellular events. In the development of holometabolous insects, a larval stage with little
46 resemblance to the adult transitions to a non-feeding pupal stage during which metamorphosis
47 takes place. This life cycle strategy arose 350 million years ago in the Carboniferous period and led
48 to the amazing radiation of the four most successful orders of insects: coleopterans, lepidopterans,
49 hymenopterans and dipterans (Truman and Riddiford, 2019). The temporal regulation of the larva-
50 pupa transition depends on hormones produced by the neuroendocrine system, chief among
51 them the steroid ecdysone, secreted by the cells of the prothoracic gland (Tennessen and
52 Thummel, 2011; Yamanaka et al., 2013). The prothoracic gland (PG) is part of the ring gland, a
53 tripartite organ situated anterior to the brain and additionally consisting of the corpus allatum
54 and the corpora cardiaca (Fig. 1A). The cells of the PG and corpus allatum have an ectodermal
55 origin in tracheal primordia of the embryonic head, whereas the corpora cardiaca derive from
56 mesoderm (Sanchez-Higueras et al., 2014). Studies in the fruit fly *Drosophila melanogaster*, a
57 dipteran, have shown that multiple molecular signals influence ecdysone production by the PG,
58 including PTTH, insulin and TOR, Hippo, TGFβ, EGF, DILP8, nitric oxide, the circadian clock,
59 ecdysone itself, tyramine, serotonin and Hh (Texada et al., 2020). Their coordinated actions on PG
60 cells integrate developmental inputs and environmental cues to determine the timing of ecdysone
61 synthesis and release. Although usually less pronounced, similar hormonally controlled
62 developmental transitions are common in animal development. Indeed, puberty transition and
63 insect metamorphosis might share a common Urbilaterian ancestry (Barredo et al., 2021). In
64 general, hormonal control of developmental timing and transitions maximizes organismal fitness
65 by ensuring development that is reproducible, robust and adjusted to conditions external to it,
66 such as resource availability, environmental insults and damage to the organism.

67 Tissue damage signaling activated by mechanical wounding (Bryant, 1971; Díaz-García and
68 Baonza, 2013) or high levels of cell death (Akai et al., 2021; Hackney et al., 2012; Simpson and
69 Schneiderman, 1975; Smith-Bolton et al., 2009; Stieper et al., 2008) is well known to delay the
70 onset of metamorphosis. Damage-induced extension of the larval period may have evolved to
71 allow for more complete healing and regeneration before transition to the next developmental
72 stage occurs (Hariharan and Serras, 2017). Tumorous growth perturbations, sharing tissue
73 damage inflammatory mechanisms with wounds (Pastor-Pareja et al., 2008; Pastor-Pareja and Xu,

74 2013), delay or completely inhibit the larva-pupa transition as well (Menut et al., 2007; Pagliarini
75 and Xu, 2003; Sehnal and Bryant, 1993). One of the signals mediating damage-induced
76 metamorphosis delay is the biosynthesis of retinoids (Halme et al. 2010). Through poorly
77 understood mechanisms, retinoids inhibit production in the central nervous system of
78 prothoracicotropic hormone (PTTH), required for ecdysone production by the PG. Another signal
79 acting on PG ecdysone production through inhibition of PTTH synthesis is Dilp8, a member of the
80 insulin-like/relaxin family of peptide hormones. Dilp8 is produced by damaged tissues and tumors
81 downstream of the c-Jun N-terminal kinase (JNK) pathway (Colombani et al., 2012; Garelli et al.,
82 2012). Autocrine JAK/STAT signaling, activated in wounds and tumors by JNK-induced expression
83 of Upd cytokines (Pastor-Pareja et al., 2008; Wu et al., 2010), has been reported to enhance local
84 Dilp8 production by the damaged tissue (Katsuyama et al., 2015). In the tissue damage response,
85 however, JAK/STAT-activating Upd cytokines have been shown to act not just locally, driving
86 damage-induced regenerative growth (Katsuyama et al., 2015; La Fortezza et al., 2016;
87 Santabarbara-Ruiz et al., 2015; Wu et al., 2010), but also systemically. Indeed, damaged-induced
88 Upd cytokines mediate an innate immune response that induces proliferation of circulating
89 macrophages and amplifies itself through additional Upd cytokine expression in the fat body
90 (Pastor-Pareja et al., 2008). Furthermore, Upd cytokines have been shown to act systemically as
91 well for inter-organ communication of nutritional status in the adult (Rajan and Perrimon, 2012).
92 Additional, non-local roles of damage-induced Upd cytokines in developmental timing are
93 therefore possible.

94 The JAK/STAT (Janus kinase and signal transducer and activator of transcription) signaling pathway
95 (Fig. 1B), is a major mediator of innate immune responses in vertebrates and insects alike (Agaisse
96 and Perrimon, 2004; Lemaitre and Hoffmann, 2007). In *Drosophila*, JAK/STAT signaling is activated
97 by three highly similar Interleukin-6-related cytokine ligands: Unpaired (Upd) (Harrison et al.,
98 1998), Upd2 (Gilbert et al., 2005; Hombría et al., 2005) and Upd3 (Agaisse et al., 2003). Upd
99 cytokines bind to the transmembrane receptor Domeless (Dome) (Brown et al., 2001; Chen et al.,
100 2002), inducing activation of the receptor-associated Janus kinase (JAK) homolog Hopscotch (Hop)
101 (Binari and Perrimon, 1994). Activated Hop in turn phosphorylates STAT transcription factor
102 homolog Stat92E (Hou et al., 1996; Yan et al., 1996), which then translocates as a dimer to the
103 nucleus to activate expression of target genes (Arbouzova and Zeidler, 2006; Rawlings et al., 2004;
104 Zeidler and Bausek, 2013). In addition to its immune roles, JAK/STAT activation by Upd cytokines

105 is pleiotropically involved in normal development and differentiation of multiple non-immune
106 organs and cell types in *Drosophila*. Examples of non-immune contexts where JAK/STAT signaling
107 is known to play a developmental role include segmental patterning (Binari and Perrimon, 1994),
108 tracheae (Brown et al., 2001), border cells of the ovarian follicle (Beccari et al., 2002; Silver and
109 Montell, 2001), the eye (Zeidler et al., 1999), the wing (Recasens-Alvarez et al., 2017), the optic
110 lobe (Yasugi et al., 2008), and multiple stem cell niches (Herrera and Bach, 2019). A systemic
111 JAK/STAT immune response, such as the tissue damage response, may therefore influence
112 development of multiple tissues. Whether the inflammatory and developmental functions of
113 JAK/STAT signaling intersect, however, has not been investigated.

114 Here, we studied the role of JAK/STAT signaling in the PG. We found that JAK/STAT signaling is
115 active during normal PG development. Reduced JAK/STAT signaling decreased average PG size
116 and slightly advanced metamorphosis, while pathway hyperactivation caused PG hypertrophy
117 and delayed the larva/pupa transition. Tissue damage and tumors, known to secrete Upd
118 cytokines, also led to JAK/STAT activation in the PG and metamorphosis delay. JAK/STAT effects
119 on the PG, our results indicate, are mediated at least in part by downstream expression of Apontic.
120 Altogether, our experiments reveal that damage signaling by Upd cytokines regulates the onset
121 metamorphosis by directly activating JAK/STAT signaling in the PG, thus coopting a developmental
122 role of JAK/STAT therein.

123

124 **RESULTS**

125 **Intrinsic JAK/STAT signaling modulates PG growth and metamorphosis**

126 To investigate a possible role of JAK/STAT signaling in ring gland development and developmental
127 timing, we examined expression of 10xSTAT-GFP, a reporter of JAK/STAT signaling in which GFP
128 expression is driven by 10 copies of the STAT binding sequence in the promoter of JAK/STAT target
129 *Socs36E* (Ekas et al., 2006). In ring glands dissected from wandering third instar larvae (wL3), we
130 were able to detect expression of the STAT-GFP reporter in the prothoracic gland (PG), increased
131 when two copies of the reporter were present in homozygous flies (Fig. 1C). In addition, we found
132 that reporters *dome-GAL4* and *upd3-GAL4*, transcriptional reporters for the expression of
133 *domeless*, encoding the JAK/STAT receptor, and *unpaired3*, encoding one of the three JAK/STAT-

134 activating, Interleukin-6-related cytokines present in *Drosophila*, were expressed in the PG as well
135 (Fig. 1D), further suggesting that JAK/STAT signaling is active in the PG. To test a role of JAK/STAT
136 signaling in the PG, we examined ring glands in different conditions affecting JAK/STAT signaling.
137 Knock down of the genes encoding receptor Domeless, the kinase Hopscotch and transcription
138 factor Stat92E under control of PG-specific *phm-GAL4*, as well as expression of dominant negative
139 Domeless (Dome$^{\Delta CYT}$), resulted in ring glands that were in average smaller than controls (Fig. 1E
140 and F, quantified in Fig. 1J). Among the three JAK/STAT ligands, knock down of *upd3* with two
141 different RNAi transgenes showed a consistent decrease on ring gland size (Fig. 1E, F and J), while
142 knock down of *upd* and *upd2* had not significant or less significant effects. Furthermore, null *upd3*
143 mutants (Osman et al., 2012) also showed significantly reduced PG size (Fig. 1G-I). Because the
144 PG has a major role in regulating developmental timing, we next investigated the effect of
145 JAK/STAT signaling reduction in the timing of the larva/pupa transition. To do that, we recorded
146 the time of pupation of animals after L1 ecdysis (embryo/L1 transition). Compared to controls, we
147 observed that the time of the larva/pupa transition was advanced in different JAK/STAT loss of
148 function conditions, with *upd3* null mutants and Dome$^{\Delta CYT}$ expression in the PG showing the
149 clearest such advanced pupation effects (Fig. 1K). In all, these results indicate that intrinsically-
150 activated JAK/STAT signaling is active in the PG, where it contributes to its development and
151 modulates the timing of the larva/pupa transition.

152 **JAK/STAT hyperactivation in the PG delays metamorphosis**

153 To further investigate the role of JAK/STAT signaling in the PG, we aimed at increasing JAK/STAT
154 activity and studying its effects on PG development and metamorphosis onset. To do that, we
155 overexpressed JAK/STAT cytokines Upd, Upd2 and Upd3 in the PG under control of *phm-GAL4*.
156 We found that expression of all three cytokines showed similar ability to activate JAK/STAT
157 signaling, as evidenced by highly increased expression of the 10xSTAT-GFP activity reporter (Fig.
158 2A, quantified in Fig. 2B). In addition to this, we observed that larvae expressing JAK/STAT
159 cytokines in their PG did not pupate and became giant larvae (Fig. 2C). The PG in these larvae, and
160 in larvae overexpressing Dome and Hop in their PG, became highly enlarged and abnormal, with
161 some cells presenting a large degree of vacuolation (Fig. 2D and E), suggestive of a degenerative
162 or autolytic process. PG hypertrophy was accompanied by a spectacular increase in nuclear size
163 and ploidy of these cells estimated by their DNA content, while average PG ploidy was reduced
164 upon knock down of *Stat92E* (Fig. 2F). The number of PG nuclei in JAK/STAT loss (*phm>Stat92E^{i}*)

165 and gain (*phm>upd*^{OE}) conditions, however, did not change with respect to the wild type (Fig. 2G).
166 Consistent with their inability to undergo larva/pupa transition, quantitative real time PCR
167 showed that the PG of animals overexpressing Upd expressed reduced levels of *disembodied* (*dib*),
168 *neverland* (*nvd*), *phantom* (*phm*) and *shadow* (*sad*), encoding Halloween group enzymes, involved
169 in the synthesis of ecdysone (Fig. 2H, results of three biological replicates). All these results
170 support a positive role of JAK/STAT signaling in PG cell growth and endoreplication. At the same
171 time, they indicate that while basal levels of JAK/STAT signaling counter premature
172 metamorphosis, JAK/STAT hyperactivation has the opposite effect and prevents pupation.

173 We were intrigued by the JAK/STAT hyperactivation PG phenotype combining enlargement and
174 partial tissue destruction. We found in the literature a strikingly similar phenotype caused by loss
175 of function of *smt3*, encoding the *Drosophila* homolog of Ubiquitin-like posttranslational modifier
176 SUMO (Talamillo et al., 2008). Furthermore, the E3 SUMO ligase Su(var)2-10, also known as PIAS
177 (Protein Inhibitor of Activated STATs), regulates STAT activity in *Drosophila* and humans (Betz et
178 al., 2001; Grönholm et al., 2010). We found that knock down of *smt3*, *Su(var)2-10* and other
179 components of the *Drosophila* SUMOylation cascade strongly increased JAK/STAT activity in the
180 ring gland, evidenced by increased 10xSTAT-GFP reporter expression (Fig. 3A, quantified in Fig.
181 3B). Extreme PG hypertrophy was observed with RNAi transgenes targeting *Su(var)2-10* (Fig. 3A,
182 quantified in Fig. 3C), producing in addition inhibition of the larva/pupa transition (Fig. 3D).
183 Confirming that SUMOylation affects PG development through JAK/STAT hyperactivation, knock
184 down of *Stat92E* strongly suppressed JAK/STAT activity and hypertrophy in the PG induced by
185 *Su(var)2-10* knock down (Fig. 3E, quantified in Fig. 3F and 3G). Furthermore, *Stat92E* knock down
186 allowed development of these animals into adults (Fig. 3H and I). These results indicate that
187 JAK/STAT activity in the PG is negatively regulated by the SUMOylation cascade and confirm the
188 potential of the JAK/STAT pathway to influence PG development and timing of metamorphosis.

189 **Tumors and tissue damage activate PG-extrinsic JAK/STAT signaling to delay metamorphosis**

190 Upd cytokines are abundantly produced in innate immune responses (Agaisse and Perrimon,
191 2004). Of note, Upd cytokines produced by tumors or wounds have been previously shown to
192 activate JAK/STAT signaling in the fat body and blood cells, causing a systemic response through
193 fat body amplification of cytokine production (Pastor-Pareja et al., 2008). Since we had found that
194 JAK/STAT activity regulated pupation time in the PG, we hypothesized that extrinsically produced

195 Upd cytokines could act in the PG similar to intrinsically expressed ones. To test this, we
196 overexpressed cytokines Upd1, Upd2 and Upd3 outside the PG under control of *Cg-GAL4*,
197 expressed in the fat body and circulating blood cells of the hemolymph-filled body cavity (Fig. 4A).
198 In all three cases, we found that PG-extrinsic expression of Upd cytokines was capable of inducing
199 high levels of 10xSTAT-GFP reporter expression in the PG (Fig. 4B, quantified in Fig. 4C).
200 Furthermore, these animals showed absent or delayed metamorphosis (Fig. 4D and E). These
201 results, importantly, show that Upd cytokines produced outside of the PG can activate JAK/STAT
202 signaling and produce developmental delay, similar to that observed when Upd cytokines were
203 overexpressed by PG cells or when activity of the pathway was manipulated inside the PG.

204 Having shown that extrinsically produced Upd cytokines can activate JAK/STAT signaling in the PG,
205 we asked whether tissue damage conditions elevating systemic Upd cytokine levels induced
206 JAK/STAT activity in the PG. We found that puncture wounding of the larval epidermis as well as
207 neoplastic tumors in *scribbled* (*scrib*) mutants increased JAK/STAT activity in the PG (Fig. 5A,
208 quantified in Fig. 5B), suggesting that upon tissue damage, JAK/STAT activation in the PG could
209 contribute to metamorphosis delay in these conditions. To test this, we employed a mosaic model
210 of clonally-induced tumors in the wing imaginal discs. In this model, large tumors formed by
211 *scribbled warts* (*scrib wts*) homozygous double mutant cells are generated through mitotic
212 recombination in a wild type animal (Fig. 5C). Despite pupation delay by *scrib wts* wing disc tumors,
213 all animals in the end are capable of undergoing metamorphosis. In this tumor model, we found
214 that activation of JAK/STAT signaling in the PG was decreased by expression of dominant negative
215 receptor Dome$^{\Delta CYT}$ (Fig. 5D, quantified in Fig. 5E). Furthermore, Dome$^{\Delta CYT}$ expression in the PG
216 partially rescued pupation delay in tumor-bearing animals (Fig. 5F, four repeats of the same
217 experiment). Similarly, Dome$^{\Delta CYT}$ expression in the PG partially rescued metamorphosis delay in
218 an experiment where damage was induced by heating mid third instar larvae at 39^{0}C for 2.5 hours
219 (Fig. 5G). Altogether, these results show that JAK/STAT activation in the PG extrinsically induced
220 by tumors and tissue damage contributes to delaying the larva/pupa developmental transition.

221 **JAK/STAT activation upregulates Apontic in the PG**

222 To further investigate the action of JAK/STAT in the ring gland, we searched for known targets of
223 JAK/STAT signaling that were expressed in the PG. We found one such candidate in Apontic, highly
224 present in the PG according to published images (Rodrigues et al., 2021). Apontic (Apt), also

225 known as Tracheae defective, is a transcription factor known to act as a downstream target of
226 JAK/STAT in border cell migration (Starz-Gaiano et al., 2008). It is also involved in the development
227 of multiple tissues, including the tracheal system (Eulenberg and Schuh, 1997). Staining with an
228 anti-Apt antibody (Liu et al., 2014) confirmed expression of Apt in the PG and the entire ring gland
229 (Fig. 6A). Furthermore, expression of Apt was highly upregulated in the PG in larvae containing
230 *scrib wts* wing disc tumors and upon overexpression of Upd in the PG (Fig. 6A, quantified in Fig.
231 6B), while levels in tracheae associated with the ring gland were not affected. Apontic levels in
232 the PG, in addition, were reduced upon *Stat92E* knock down in unchallenged larvae, and also in
233 larvae with tumors upon dominant negative Dome$^{\Delta CYT}$ expression (Fig. 6A and B). All these results
234 indicate that Apt expression is under JAK/STAT regulation in the PG.

235 To test the effect of Apt upregulation, we overexpressed Apt in the PG. Apt overexpression under
236 control of *phm-GAL4* produced larvae that did not progress beyond the L2 stage. However, when
237 expression was restricted to the L2 and L3 stages by using the GAL80ts system, we observed
238 hypertrophied PGs with enlarged nuclei (Fig. 6D and E) and inhibition of the larva/pupa transition
239 (Fig. 6F), similar to the effect of JAK/STAT hyperactivation. Apt knock down, in contrast, produced
240 slight reduction of average PG size and pupation time compared to controls (Fig. 6C and E). All
241 these results suggest that Apt may be a target mediating the effect of JAK/STAT signaling both
242 normal development and in response to tissue damage. A recent study, published while this
243 manuscript was in preparation, found microRNA *bantam* (*ban*) was upregulated downstream of
244 JAK/STAT signaling in the PG (Romão et al., 2021). We checked the effect of *ban* overexpression
245 in the PG and found that it could also induce PG overgrowth (Fig. 6G and H). However, contrary
246 to Apt expression, *ban*-overexpressing PGs contained regions with large numbers of apparently
247 diploid cells, suggesting that *ban* upregulation can increase number of PG cells before
248 polyploidization and/or induce depolyploidization. Also in contrast with Apt overexpression, flies
249 overexpressing *ban* in the PG were capable of pupating and producing adults, while Apt-
250 overexpressing flies did not pupate (Fig. 6I and J). Finally, we found that the PG in larvae with *scrib*
251 *wts* wing disc tumors, similar to Upd overexpression, *Su(var)2-10* knock down and Apt
252 overexpression, presents high levels of autophagy induction, as evidenced by formation of
253 numerous large Atg.mCherry-positive vesicles in the cytoplasm, consistent with the vacuolation
254 and varying degrees of tissue degeneration in these PG, and contrary to what is observed in the
255 *ban*-overexpressing PG (Fig. 6K). Our results, therefore, suggest that different JAK/STAT targets
256 may contribute to different aspects of the response to tissue damage (Fig. 7) and leaves for future

257 studies a thorough analysis of these targets, their effects on PG development and their integration
258 with other signals regulating developmental timing.

259

260 **DISCUSSION**

261 Our results show that JAK/STAT signaling is active in the PG at low levels during normal
262 development. Another study examined JAK/STAT activity in the PG and found in it as well
263 expression of the same 10xSTAT-GFP reporter we used (Pan and O'Connor, 2020). We found, in
264 addition, that pupation is slightly advanced and the size of the ring gland is smaller in multiple
265 conditions of JAK/STAT signaling reduction, including knock down in PG cells of *upd3*, which a
266 GAL4 expression reporter shows is intrinsically expressed in the ring gland. JAK/STAT signaling
267 during embryonic development is known to be involved in the specification of the tracheal
268 primordium that gives rise to the PG and corpus allatum (Sanchez-Higueras et al., 2014). Our
269 results may therefore reveal a continued role of JAK/STAT for the development and differentiation
270 of the larval PG.

271 Consistent with a role of JAK/STAT in ring gland development, hyperactivation of the pathway
272 exhibited contrary effects, producing PG overgrowth and metamorphosis delay. PG overgrowth
273 and ploidy increase is observed in conditions hyperactivating TOR/insulin signaling (Mirth et al.,
274 2005; Ohhara et al., 2017). However, those conditions result in advanced pupation. This has been
275 interpreted as revealing a mechanism by which insulin-driven PG growth mirrors organismal
276 growth and triggers metamorphosis in well-fed animals. PG overgrowth resulting from JAK/STAT
277 activation, in stark contrast, inhibits transcription of enzymes in the ecdysone synthesis pathway
278 and results in absent or delayed metamorphosis. Also in contrast, JAK/STAT-induced PG
279 hypertrophy leads to a highly aberrant tissue where vacuolation, autophagy and large differences
280 in cell size are observed. We found in the literature that loss of *smt3*, encoding fly SUMO, caused
281 a strikingly similar PG hypertrophy phenotype (Talamillo et al., 2008). Our results, showing that
282 *Stat92E* knock down suppresses the effect of SUMO E3 ligase Su(var)2-10 knock down, indicate
283 that hyperactivation of JAK/STAT signaling is responsible for this phenotype. This suppression
284 result, in fact, further confirms a role of JAK/STAT in PG development, since PIAS has been shown
285 to specifically bind and inhibit only active phosphorylated dimeric STAT, not monomeric STAT

286 (Liao et al., 2000), and thus pathway hyperactivation in this condition strongly implies pre-existing
287 activity.

288 In addition to its developmental role, JAK/STAT signaling is activated in the PG in response to
289 tumors and tissue damage. Strong local upregulation of all three Upd cytokines has been observed
290 in tumors (Wu et al., 2010), while amplification through systemic upregulation has been observed
291 for Upd3 at least (Pastor-Pareja et al., 2008). Although not investigated here, our results predict
292 that JAK-STAT activation by infection may regulate developmental timing as well, given the
293 involvement of Upd cytokines in the immune response to pathogens (Agaisse and Perrimon, 2004).
294 A study postulated that JAK/STAT signaling influences developmental timing by enhancing local
295 expression of Dilp8 in wounded tissue (Katsuyama et al., 2015). Our results show that Upd
296 cytokines, in addition, have a strong unmediated effect in the PG, where they activate JAK/STAT
297 signaling and influence the larva/pupa transition directly. Partial rescue of tumor-induced
298 pupation delay by expressing a dominant negative version of the JAK/STAT receptor Domeless in
299 the PG clearly shows that JAK/STAT acts directly in the PG without mediation of Dilp8. Pupation
300 delays induced by tissue damage are only partially rescued in null mutants for *Lgr3* (Garelli et al.,
301 2015), encoding the specific receptor of Dilp8, which suggests that JAK/STAT, Dilp8 and perhaps
302 other signals may be responsible for damage-induced pupation delay in parallel.

303 A number of pathway ligands acting in tissues in typical developmental patterning and
304 differentiation/growth capacities have been shown to regulate ecdysone production by the PG.
305 Such is the case of Hedgehog, released from enterocytes under starvation conditions (Rodenfels
306 et al., 2014). TGFβ homolog Dpp, normally escaping from imaginal discs to the hemolymph (Ma
307 et al., 2017), has been shown to downregulate ecdysone production by increasing nuclear FOXO
308 localization and *ban* expression, suggesting that disc-derived Dpp functions as a signal that
309 conveys organismal growth status to the endocrine system (Setiawan et al., 2018). Because Upd
310 cytokines are produced during normal development in multiple organs, including imaginal discs,
311 it is possible that PG-extrinsic Upd expression also serves a coordination role in normal
312 development similar to Dpp. More recently, EGF ligands Spitz and Vein expressed intrinsically in
313 the PG have been shown to regulate pupation as well, in this case stimulating ecdysone
314 production (Cruz et al., 2020). This raises the converse question of whether EGF produced by
315 other tissues can influence timing of the larva/pupa transition. Altogether, these studies paint a
316 scenario in which the distinction between short-range developmental pathway ligands, long-

317 range inter-organ communication hormones and immune response cytokines becomes
318 increasingly blurred.

319 While we were finishing our study, the group of Marco Milan reported that Upd3 signals from the
320 tumor to the PG to delay metamorphosis (Romão et al., 2021), consistent with our findings.
321 According to that study, JAK/STAT inhibits pupation by inducing expression of the *ban* miRNA. Our
322 study confirms the ability of Upd cytokines from damaged tissue to delay pupation while, in
323 addition, showing that Apontic is a target of JAK/STAT signaling in the PG. The effects of Apontic,
324 indeed, closely resembled those of JAK/STAT hyperactivation achieved through Upd
325 overexpression or *Su(var)2-10* knock down, including tissue hypertrophy and autophagy. The
326 response to JAK/STAT in the PG, therefore, is likely to involve multiple targets. Future studies
327 should clarify the targets and mechanisms by which JAK/STAT signaling regulates developmental
328 timing by the PG.

329 **MATERIALS AND METHODS**

330 ***Drosophila* strains and genetics**

331 Standard fly husbandry techniques and genetic methodologies were used to assess segregation
332 of transgenes in the progeny of crosses, construct intermediate strains and obtain flies of the
333 desired genotypes for each experiment (Roote and Prokop, 2013). The GAL4-UAS binary
334 expression system (Brand and Perrimon, 1993) was used to drive expression of UAS transgenes
335 under control of GAL4 drivers *phm-GAL4* (PG) and *Cg-GAL4* (fat body). Flies were reared at 25°C
336 on standard fly medium in all experiments, except for *apt* overexpression experiments using the
337 $GAL80^{ts}$ thermosensitive GAL4 repressor (McGuire et al., 2003), in which crosses to obtain
338 $phm^{ts}>apt^{OE}$ animals were left for three days at 18°C to avoid early lethality before transferring to
339 30°C. Genotypes of flies in all experiments are detailed in Table S1. Original fly strains used in this
340 study are listed in Table S2.

341 **Imaging and image analysis**

342 Ring glands and wing discs were predissected in PBS by turning larvae inside out with fine tip
343 forceps, fixed in PBS containing 4% PFA (paraformaldehyde, Sinopharm Chemical Reagent, cat #
344 80096692), washed in PBS (3 × 10 min), dissected from the carcass and mounted on a glass slide
345 with a drop of DAPI-Vectashield (Vector Laboratories, cat # H-1200). Confocal images were
346 acquired with a Zeiss LSM780 confocal microscope equipped with Plan-Apochromat 20× NA 0.8
347 objective (ring gland images) and an EC Plan-Neofluar 10× NA 0.3 objective (wing disc images).
348 Images of larvae, pupae and adults were taken with a Leica M125 stereomicroscope, except for
349 the image in Fig. 4A, taken with a Leica MZ10F stereomicroscope.

350 For quantification of JAK/STAT activity in the PG, the polygon selection in ImageJ-FIJI software was
351 used to outline the area occupied by the PG in confocal images of ring glands and mean 10xSTAT-
352 GFP intensity (total fluorescence intensity divided by area) was measured inside. At least five ring
353 glands were analysed in each condition.

354 For PG size quantification, the polygon selection in ImageJ-FIJI software was used to measure the
355 area occupied by the PG in confocal images of ring glands. At least five ring glands were analyzed
356 for each condition (each point represents the PG size in one ring gland).

357 For PG nuclear counts, nuclei were manually counted using the Multiple points tool in ImageJ-FIJI
358 software. These counts were conducted on confocal Z-stack images of DAPI and CD8.GFP
359 (expressed under PG-specific *phm-GAL4* control). At least 18 ring glands were analysed per
360 genotype.

361 For ploidy estimation, ring glands from wL3 larvae were dissected, fixed and mounted in DAPI-
362 Vectashield (Vector Labs). Z-stacks of images of DAPI and *phm-GAL4*-driven CD8.GFP were
363 acquired in a Zeiss LSM780 confocal microscope equipped with a Plan-Apochromat 63X oil
364 objective. On those stacks, the volume of PG nuclei was delimited and labelled with the Surface
365 function in Imaris 9.3.1 software (Bitplane) and total DAPI fluorescence inside the nucleus
366 recorded. Ploidy was calculated with reference to the average value in measurements of DAPI
367 fluorescence conducted in the same way in diploid (2C) blood cells.

368 For quantification of anti-Apt signal, the polygon selection in ImageJ-FIJI software was used to
369 outline the PG nuclei in confocal images of stained ring glands and mean intensity (total
370 fluorescence intensity divided by area) was measured inside. More than 120 PG nuclei from at
371 least 8 ring glands were analysed for each genotype.

372 **Immunohistochemistry**

373 Anti-Apt stainings were performed following standard procedures for imaginal discs. Briefly, wL3
374 larvae were pre-dissected in PBS by turning them inside-out with fine tip forceps, fixed in 4% PFA
375 for 15 min, washed in PBS (3 x 15 min), blocked in PBT-BSA (PBS containing 0.1% Triton X-100
376 detergent, 1% BSA, and 250 mM NaCl), incubated overnight with primary anti-Apt in PBT-BSA at
377 4^0C, washed in PBT-BSA (3 x 20 min), incubated for 2 h with anti-rabbit IgG conjugated to Alexa-
378 555 (1:200, Life Technologies) in PBT-BSA at room temperature, and washed in PBT-BSA (3 x 10
379 min) and PBS (3 x 10 min). Stained ring glands were finally dissected and mounted on a slide with
380 a drop of DAPI-Vectashield (Vector Labs).

381 **Pupation timing**

382 Fresh virgin female and male flies were kept together in bottles 3 days for mating and then
383 allowed to lay eggs onto grape juice agar plates for 2 h at 25°C. The next day, newly hatched first
384 instar larvae (L1) were picked at 1 h intervals and transferred to standard medium vials on which

385 the top layer of food had been ground with forceps. 20 to 40 larvae were deposited in each vial.
386 The number of pupated animals was counted at 2 to 6 h intervals. For the experiment in Fig. 6I,
387 egg laying took place during 1 day in regular food vials instead and pupation time was computed
388 in days after egg laying (±0.5 days).

389 **Quantitative RT-PCR**

390 Total RNA was extracted from cephalic complexes containing the ring gland using TRIzol reagent
391 (ThermoFisher Scientific), treated with DNase (Promega) and used as a template for cDNA
392 synthesis using iScript™ cDNA Synthesis Kits (BIO-RAD). RT-PCR reactions were performed using
393 SYBR Green Supermix (BIO-RAD) in a CFX96 Real-Time PCR system (BIO-RAD). Expression values
394 were normalized to *rpL23* transcript levels. Fold change with respect to the wild type control was
395 calculated with Bio-Rad CFX Manager 3.1 software. Three separate biological replicates were
396 performed for each experiment, each with three technical replicates. Primers used were:

397 rpL23-F: GACAACACCGGAGCCAAGAACC, rpL23-R: GTTTGCGCTGCCGAATAACCAC;
398 phm-F: GGATTTCTTTCGGCGCGATGTG, phm-R: TGCCTCAGTATCGAAAAGCCGT;
399 dib-F: TGCCCTCAATCCCTATCTGGTC, dib-R: ACAGGGTCTTCACACCCATCTC;
400 sad-F: CCGCATTCAGCAGTCAGTGG, sad-R: ACCTGCCGTGTACAAGGAGAG;
401 nvd-F: GGAAGCGTTGCTGACGACTGTG, nvd-R: TAAAGCCGTCCACTTCCTGCGA.

402 **Wounding assay**

403 Wounding of the larval epidermis was performed on mid L3 larvae by puncturing at once dorsal
404 and ventral epidermis near the posterior end of the larva with fine tip forceps. Wounding
405 operations were perfomed on sylgard plates on clean, dried larvae, avoiding damage to the gut
406 or other internal organs. Operated larvae were kept on a dry slide for 5 min to allow coagulation
407 at the wound and prevent bleeding. Operated larvae were finally transferred to standard medium
408 vials on which the top layer of food had been ground with forceps.

409 **Heating assay**

410 Newly hatched L1 larvae were picked at 1 h intervals and transferred to standard food vials after
411 4 h egg laying in agar juice plates, placing 20 to 40 animals per vial. 4 days after L1 ecdysis, mid L3
412 larvae were picked and transferred into 3.5-cm plastic dishes filled with ground standard food for

413 heat treatment. The dishes were sealed with parafilm and placed for 2.5 hours in a water bath at
414 25°C (control) or 39°C. After heating, larvae were kept at room temperature for 15 min and then
415 placed back into standard food vials in which the top layer of food had been ground with forceps.
416 Pupation time after L1 ecdysis was recorded.

417 **Quantification and statistical analysis**

418 Statistical analysis and graphical representations were performed with Graphpad Prism software.
419 Horizontal lines in all graphs represent average values (means). For statistical comparisons,
420 unpaired two-tailed Student's t tests were conducted when data passed both D'Agostino-Pearson
421 normality tests and F-tests for equal variance. Unpaired two-tailed t-tests with Welch's correction
422 were used when data passed D'Agostino-Pearson normality tests, but not F-tests for equal
423 variance. Finally, non-parametric Mann-Whitney tests were used when data did not pass
424 D'Agostino-Pearson normality tests. Significance of statistical tests is reported in graphs as follows:
425 $p<0.0001$ (****), $p<0.001$ (***), $p<0.01$ (**), $p<0.05$ (*), and $p>0.05$ (n.s., not significant).

426 **ACKNOWLEDGMENTS**

427 We thank Francisco Martin, Tian Xu, Jian-Quan Ni, James Castelli-Gair Hombria, Zhouhua Li, Herve
428 Agaisse, the Tsinghua Fly Center, Bloomington Drosophila Stock Center, Vienna Drosophila
429 Research Center and Kyoto National Institute of Genetics for fly strains, and Qing-Xin Liu for anti-
430 Apontic antibody. We also thank Marta Rojas for assistance with RNA extraction and qRT-PCR.
431 This research was supported by grants 31771600 and 91854207 from the Natural Science
432 Foundation of China (NSFC).

433

434 **Competing interests**

435 No competing interests declared.

436 **REFERENCES**

437 **Agaisse, H. and Perrimon, N.** (2004). The roles of JAK/STAT signaling in Drosophila
438 immune responses. *Immunol Rev* **198**, 72-82.

439 **Agaisse, H., Petersen, U. M., Boutros, M., Mathey-Prevot, B. and Perrimon, N.** (2003).
440 Signaling role of hemocytes in Drosophila JAK/STAT-dependent response to septic injury.
441 *Dev Cell* **5**, 441-50.

442 **Akai, N., Ohsawa, S., Sando, Y. and Igaki, T.** (2021). Epithelial cell-turnover ensures robust
443 coordination of tissue growth in Drosophila ribosomal protein mutants. *PLoS Genet* **17**,
444 e1009300.

445 **Arbouzova, N. I. and Zeidler, M. P.** (2006). JAK/STAT signalling in Drosophila: insights into
446 conserved regulatory and cellular functions. *Development* **133**, 2605-16.

447 **Barredo, C. G., Gil-Marti, B., Deveci, D., Romero, N. M. and Martin, F. A.** (2021). Timing
448 the Juvenile-Adult Neurohormonal Transition: Functions and Evolution. *Front Endocrinol*
449 **11**, 602285.

450 **Beccari, S., Teixeira, L. and Rørth, P.** (2002). The JAK/STAT pathway is required for border
451 cell migration during Drosophila oogenesis. *Mech Dev* **111**, 115-23.

452 **Betz, A., Lampen, N., Martinek, S., Young, M. W. and Darnell, J. E., Jr.** (2001). A
453 Drosophila PIAS homologue negatively regulates stat92E. *Proc Natl Acad Sci U S A* **98**,
454 9563-8.

455 **Binari, R. and Perrimon, N.** (1994). Stripe-specific regulation of pair-rule genes by
456 hopscotch, a putative Jak family tyrosine kinase in Drosophila. *Genes Dev* **8**, 300-312.

457 **Brand, A. H. and Perrimon, N.** (1993). Targeted gene expression as a means of altering
458 cell fates and generating dominant phenotypes. *Development* **118**, 401-15.

459 **Brown, S., Hu, N. and Hombría, J. C.** (2001). Identification of the first invertebrate
460 interleukin JAK/STAT receptor, the Drosophila gene domeless. *Curr Biol* **11**, 1700-5.

461 **Bryant, P. J.** (1971). Regeneration and duplication following operations in situ on the
462 imaginal discs of Drosophila melanogaster. *Dev Biol* **26**, 637-651.

463 **Chen, H. W., Chen, X., Oh, S. W., Marinissen, M. J., Gutkind, J. S. and Hou, S. X.** (2002).
464 mom identifies a receptor for the Drosophila JAK/STAT signal transduction pathway and
465 encodes a protein distantly related to the mammalian cytokine receptor family. *Genes*
466 *Dev* **16**, 388-98.

467 **Colombani, J., Andersen, D. S. and Leopold, P.** (2012). Secreted peptide Dilp8 coordinates
468 Drosophila tissue growth with developmental timing. *Science* **336**, 582-5.

469 **Cruz, J., Martín, D. and Franch-Marro, X.** (2020). Egfr Signaling Is a Major Regulator of
470 Ecdysone Biosynthesis in the Drosophila Prothoracic Gland. *Curr Biol* **30**, 1547-1554.e4.

471 **Díaz-García, S. and Baonza, A.** (2013). Pattern reorganization occurs independently of cell
472 division during Drosophila wing disc regeneration in situ. *Proc Natl Acad Sci U S A* **110**,
473 13032-13037.

474 **Ekas, L. A., Baeg, G. H., Flaherty, M. S., Ayala-Camargo, A. and Bach, E. A.** (2006).
475 JAK/STAT signaling promotes regional specification by negatively regulating wingless
476 expression in Drosophila. *Development* **133**, 4721-9.

477 **Eulenberg, K. G. and Schuh, R.** (1997). The tracheae defective gene encodes a bZIP
478 protein that controls tracheal cell movement during Drosophila embryogenesis. *EMBO J*
479 **16**, 7156-65.

480 **Garelli, A., Gontijo, A. M., Miguela, V., Caparros, E. and Dominguez, M.** (2012). Imaginal
481 discs secrete insulin-like peptide 8 to mediate plasticity of growth and maturation. *Science*
482 **336**, 579-82.

483 **Garelli, A., Heredia, F., Casimiro, A. P., Macedo, A., Nunes, C., Garcez, M., Dias, A. R. M.,**
484 **Volonte, Y. A., Uhlmann, T., Caparros, E. et al.** (2015). Dilp8 requires the neuronal relaxin
485 receptor Lgr3 to couple growth to developmental timing. *Nat Commun* **6**, 8732.

486 **Gilbert, M. M., Weaver, B. K., Gergen, J. P. and Reich, N. C.** (2005). A novel functional
487 activator of the Drosophila JAK/STAT pathway, unpaired2, is revealed by an in vivo
488 reporter of pathway activation. *Mech Dev* **122**, 939-948.

489 **Grönholm, J., Ungureanu, D., Vanhatupa, S., Rämet, M. and Silvennoinen, O.** (2010).
490 Sumoylation of Drosophila Transcription Factor STAT92E. *J Innate Immunity* **2**, 618-624.

491 **Hackney, J. F., Zolali-Meybodi, O. and Cherbas, P.** (2012). Tissue Damage Disrupts
492 Developmental Progression and Ecdysteroid Biosynthesis in Drosophila. *PLoS One* **7**,
493 e49105.

494 **Hariharan, I. K. and Serras, F.** (2017). Imaginal disc regeneration takes flight. *Curr Opinion*
495 *Cell Biol* **48**, 10-16.

496 **Harrison, D. A., McCoon, P. E., Binari, R., Gilman, M. and Perrimon, N.** (1998). Drosophila
497 unpaired encodes a secreted protein that activates the JAK signaling pathway. *Genes Dev*
498 **12**, 3252-3263.

499 **Herrera, S. C. and Bach, E. A.** (2019). JAK/STAT signaling in stem cells and regeneration:
500 from Drosophila to vertebrates. *Development* **146**.

501 **Hombría, J. C.-G., Brown, S., Häder, S. and Zeidler, M. P.** (2005). Characterisation of
502 Upd2, a Drosophila JAK/STAT pathway ligand. *Dev Biol* **288**, 420-433.

503 **Hou, X. S., Melnick, M. B. and Perrimon, N.** (1996). marelle acts downstream of the
504 Drosophila HOP/JAK kinase and encodes a protein similar to the mammalian STATs. *Cell*
505 **84**, 411-419.

506 **Katsuyama, T., Comoglio, F., Seimiya, M., Cabuy, E. and Paro, R.** (2015). During
507 Drosophila disc regeneration, JAK/STAT coordinates cell proliferation with Dilp8-
508 mediated developmental delay. *Proc Natl Acad Sci U S A* **112**, E2327-36.

La Fortezza, M., Schenk, M., Cosolo, A., Kolybaba, A., Grass, I. and Classen, A. K. (2016). JAK/STAT signalling mediates cell survival in response to tissue stress. *Development* **143**, 2907-19.

Lemaitre, B. and Hoffmann, J. (2007). The host defense of Drosophila melanogaster. *Annu Rev Immunol* **25**, 697-743.

Liao, J., Fu, Y. and Shuai, K. (2000). Distinct roles of the NH2- and COOH-terminal domains of the protein inhibitor of activated signal transducer and activator of transcription (STAT) 1 (PIAS1) in cytokine-induced PIAS1-Stat1 interaction. *Proc Natl Acad Sci U S A* **97**, 5267-72.

Liu, Q.-X., Wang, X.-F., Ikeo, K., Hirose, S., Gehring, W. J. and Gojobori, T. (2014). Evolutionarily conserved transcription factor Apontic controls the G1/S progression by inducing cyclin E during eye development. *Proc Natl Acad Sci U S A* **111**, 9497-9502.

Ma, M., Cao, X., Dai, J. and Pastor-Pareja, J. C. (2017). Basement Membrane Manipulation in Drosophila Wing Discs Affects Dpp Retention but Not Growth Mechanoregulation. *Dev Cell* **42**, 97-106 e4.

McGuire, S. E., Le, P. T., Osborn, A. J., Matsumoto, K. and Davis, R. L. (2003). Spatiotemporal rescue of memory dysfunction in Drosophila. *Science* **302**, 1765-8.

Menut, L., Vaccari, T., Dionne, H., Hill, J., Wu, G. and Bilder, D. (2007). A Mosaic Genetic Screen for Drosophila Neoplastic Tumor Suppressor Genes Based on Defective Pupation. *Genetics* **177**, 1667-1677.

Mirth, C., Truman, J. W. and Riddiford, L. M. (2005). The role of the prothoracic gland in determining critical weight for metamorphosis in Drosophila melanogaster. *Curr Biol* **15**, 1796-807.

Ohhara, Y., Kobayashi, S. and Yamanaka, N. (2017). Nutrient-Dependent Endocycling in Steroidogenic Tissue Dictates Timing of Metamorphosis in Drosophila melanogaster. *PLoS Genet* **13**, e1006583.

Osman, D., Buchon, N., Chakrabarti, S., Huang, Y. T., Su, W. C., Poidevin, M., Tsai, Y. C. and Lemaitre, B. (2012). Autocrine and paracrine unpaired signaling regulate intestinal stem cell maintenance and division. *J Cell Sci* **125**, 5944-5949.

Pagliarini, R. A. and Xu, T. (2003). A genetic screen in Drosophila for metastatic behavior. *Science* **302**, 1227-31.

Pan, X. and O'Connor, M. B. (2020). Coordination among multiple receptor tyrosine kinase signals controls Drosophila developmental timing and body size. *bioRxiv*, 2020.09.01.278382.

Pastor-Pareja, J. C., Wu, M. and Xu, T. (2008). An innate immune response of blood cells to tumors and tissue damage in Drosophila. *Dis Model Mech* **1**, 144-54; discussion 153.

Pastor-Pareja, J. C. and Xu, T. (2013). Dissecting social cell biology and tumors using Drosophila genetics. *Annu Rev Genet* **47**, 51-74.

547 **Rajan, A. and Perrimon, N.** (2012). Drosophila cytokine unpaired 2 regulates physiological
548 homeostasis by remotely controlling insulin secretion. *Cell* **151**, 123-37.

549 **Rawlings, J. S., Rosler, K. M. and Harrison, D. A.** (2004). The JAK/STAT signaling pathway.
550 *J Cell Sci* **117**, 1281-3.

551 **Recasens-Alvarez, C., Ferreira, A. and Milán, M.** (2017). JAK/STAT controls organ size and
552 fate specification by regulating morphogen production and signalling. *Nat Commun* **8**,
553 13815.

554 **Rodenfels, J., Lavrynenko, O., Ayciriex, S., Sampaio, J. L., Carvalho, M., Shevchenko, A.
555 and Eaton, S.** (2014). Production of systemically circulating Hedgehog by the intestine
556 couples nutrition to growth and development. *Genes Dev* **28**, 2636-2651.

557 **Rodrigues, D., Renaud, Y., VijayRaghavan, K., Waltzer, L. and Inamdar, M. S.** (2021).
558 Differential activation of JAK-STAT signaling reveals functional compartmentalization in
559 Drosophila blood progenitors. *Elife* **10**, e61409.

560 **Romão, D., Muzzopappa, M., Barrio, L. and Milán, M.** (2021). The Upd3 cytokine couples
561 inflammation to maturation defects in Drosophila. *Curr Biol* **31**, 1780-1787.e6.

562 **Roote, J. and Prokop, A.** (2013). How to design a genetic mating scheme: a basic training
563 package for Drosophila genetics. *G3 (Bethesda)* **3**, 353-8.

564 **Sanchez-Higueras, C., Sotillos, S. and Castelli-Gair Hombria, J.** (2014). Common origin of
565 insect trachea and endocrine organs from a segmentally repeated precursor. *Curr Biol* **24**,
566 76-81.

567 **Santabarbara-Ruiz, P., Lopez-Santillan, M., Martinez-Rodriguez, I., Binagui-Casas, A.,
568 Perez, L., Milan, M., Corominas, M. and Serras, F.** (2015). ROS-Induced JNK and p38
569 Signaling Is Required for Unpaired Cytokine Activation during Drosophila Regeneration.
570 *PLoS Genet* **11**, e1005595.

571 **Sehnal, F. and Bryant, P. J.** (1993). Delayed pupariation in Drosophila imaginal disc
572 overgrowth mutants is associated with reduced ecdysteroid titer. *J Insect Physiol* **39**,
573 1051-1059.

574 **Setiawan, L., Pan, X., Woods, A. L., O'Connor, M. B. and Hariharan, I. K.** (2018). The
575 BMP2/4 ortholog Dpp can function as an inter-organ signal that regulates developmental
576 timing. *Life Sci Alliance* **1**, e201800216.

577 **Silver, D. L. and Montell, D. J.** (2001). Paracrine Signaling through the JAK/STAT Pathway
578 Activates Invasive Behavior of Ovarian Epithelial Cells in Drosophila. *Cell* **107**, 831-841.

579 **Simpson, P. and Schneiderman, H. A.** (1975). Isolation of temperature sensitive
580 mutations blocking clone development inDrosophila melanogaster, and the effects of a
581 temperature sensitive cell lethal mutation on pattern formation in imaginal discs. *Wilhelm
582 Roux Arch Dev Biol* **178**, 247-275.

583 **Smith-Bolton, R. K., Worley, M. I., Kanda, H. and Hariharan, I. K.** (2009). Regenerative
584 Growth in Drosophila Imaginal Discs Is Regulated by Wingless and Myc. *Dev Cell* **16**, 797-
585 809.

586 **Starz-Gaiano, M., Melani, M., Wang, X., Meinhardt, H. and Montell, D. J.** (2008).
587 Feedback inhibition of JAK/STAT signaling by apontic is required to limit an invasive cell
588 population. *Dev Cell* **14**, 726-738.

589 **Stieper, B. C., Kupershtok, M., Driscoll, M. V. and Shingleton, A. W.** (2008). Imaginal discs
590 regulate developmental timing in Drosophila melanogaster. *Dev Biol* **321**, 18-26.

591 **Talamillo, A., Sanchez, J., Cantera, R., Perez, C., Martin, D., Caminero, E. and Barrio, R.**
592 (2008). Smt3 is required for Drosophila melanogaster metamorphosis. *Development* **135**,
593 1659-68.

594 **Tennessen, J. M. and Thummel, C. S.** (2011). Coordinating growth and maturation -
595 insights from Drosophila. *Curr Biol* **21**, R750-R757.

596 **Texada, M. J., Koyama, T. and Rewitz, K.** (2020). Regulation of Body Size and Growth
597 Control. *Genetics* **216**, 269-313.

598 **Truman, J. W. and Riddiford, L. M.** (2019). The evolution of insect metamorphosis: a
599 developmental and endocrine view. *Philos Trans R Soc Lond B Biol Sci* **374**, 20190070.

600 **Wu, M., Pastor-Pareja, J. C. and Xu, T.** (2010). Interaction between Ras(V12) and
601 scribbled clones induces tumour growth and invasion. *Nature* **463**, 545-8.

602 **Yamanaka, N., Rewitz, K. F. and O'Connor, M. B.** (2013). Ecdysone control of
603 developmental transitions: lessons from Drosophila research. *Annu Rev Entomol* **58**, 497-
604 516.

605 **Yan, R., Small, S., Desplan, C., Dearolf, C. R. and Darnell, J. E., Jr.** (1996). Identification of
606 a Stat gene that functions in Drosophila development. *Cell* **84**, 421-30.

607 **Yasugi, T., Umetsu, D., Murakami, S., Sato, M. and Tabata, T.** (2008). Drosophila optic
608 lobe neuroblasts triggered by a wave of proneural gene expression that is negatively
609 regulated by JAK/STAT. *Development* **135**, 1471-1480.

610 **Zeidler, M. P. and Bausek, N.** (2013). The Drosophila JAK-STAT pathway. *JAK-STAT* **2**,
611 e25353-e25353.

612 **Zeidler, M. P., Perrimon, N. and Strutt, D. I.** (1999). Polarity determination in the
613 Drosophila eye: a novel role for unpaired and JAK/STAT signaling. *Genes Dev* **13**, 1342-53.

Figure 1. Intrinsic JAK/STAT signaling modulates PG growth and metamorphosis

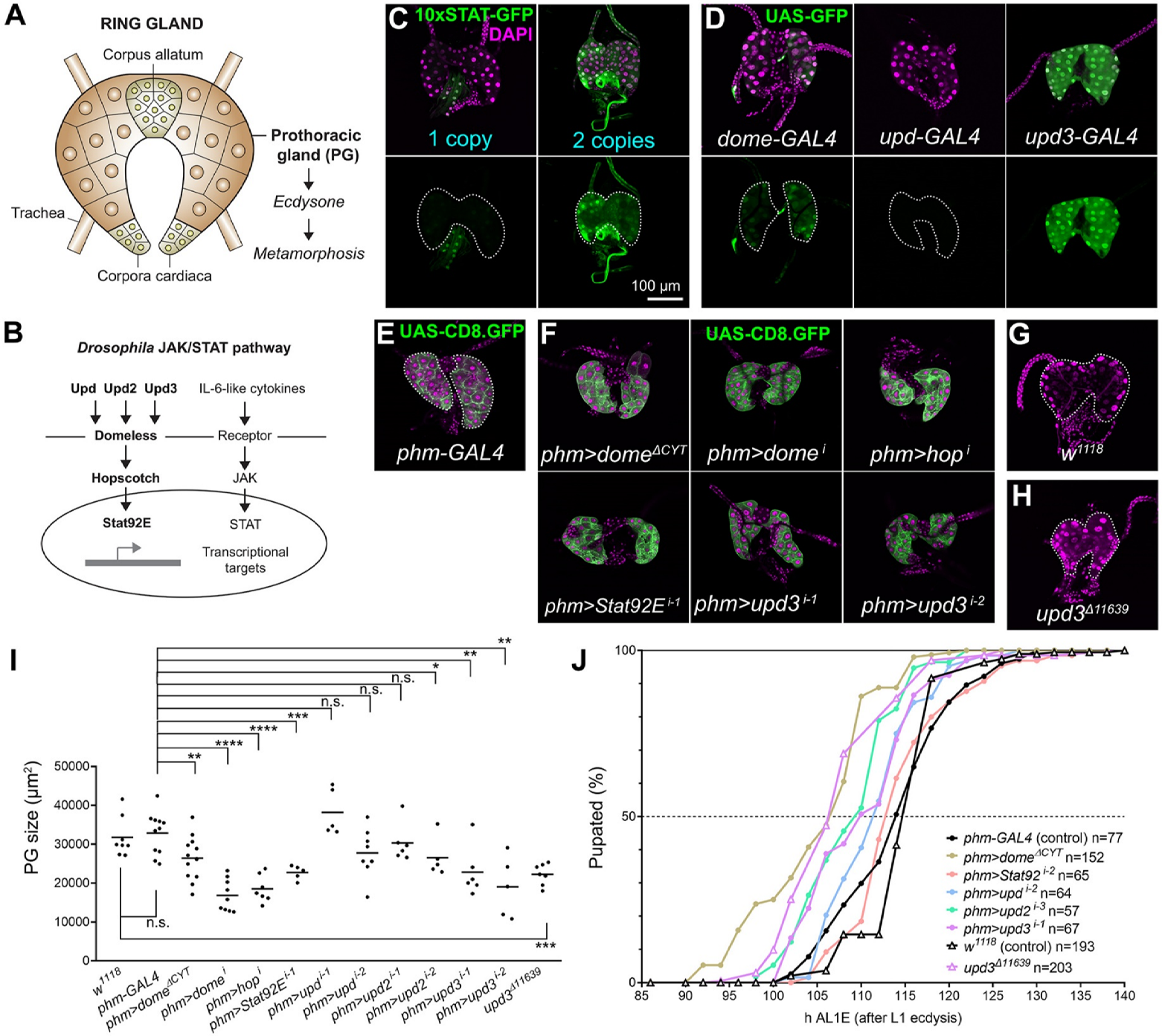

614 **Figure 1. Intrinsic JAK/STAT signaling modulates PG growth and metamorphosis**

615 (A) Schematic drawing of the ring gland of the third instar *Drosophila* larva. The prothoracic gland
616 (PG), producing ecdysone, is the largest part of this composite neuroendocrine organ.

617 (B) Components of the JAK/STAT signaling pathway in *Drosophila*.

618 (C) Confocal images of ring glands dissected from wandering third instar (wL3) larvae containing
619 one (left) or two (right) copies of the JAK/STAT activity reporter 10xSTAT-GFP (Ekas et al., 2006)
620 (green, separate channel in lower subpanels). Dotted lines represent PG outline. Nuclei stained
621 with DAPI (magenta).

622 (D) Ring glands from wL3 larvae expressing GFP (green, separate channel in lower subpanels)
623 under control of GAL4 transcriptional reporters for genes encoding receptor Domeless (left), and
624 cytokines Upd (center) and Upd3 (right). Dotted lines represent PG outline. Nuclei stained with
625 DAPI (magenta).

626 (E) Ring gland from a control wL3 larva expressing membrane GFP (CD8.GFP, green) under control
627 of PG-specific *phm-GAL4*. Dotted lines represent PG outline. Nuclei stained with DAPI (magenta).

628 (F) Ring glands from wL3 larvae expressing dominant negative Dome$^{\Delta CYT}$ or knocking down *dome*,
629 *hop*, *Stat92E* and *upd3* in the PG under control of *phm-GAL4*. Knock down of *upd3* in *phm>upd3*$^{i-1}$
630 and *phm>upd3*$^{i-2}$ experiments employs different RNAi transgenes (see Table S1 for detailed
631 genotypes in these and all other experiments throughout the manuscript). *phm-GAL4*-driven
632 CD8.GFP in green. Nuclei stained with DAPI (magenta).

633 (G) Ring gland from a *w*^{1118} control wL3 larva. Dotted lines represent PG outline. Nuclei stained
634 with DAPI (magenta).

635 (H) Ring gland from a null *upd3*$^{\Delta 11639}$ mutant wL3 larva. Dotted lines represent PG outline. Nuclei
636 stained with DAPI (magenta).

637 (I) Quantification of wL3 PG size in *phm-GAL4* and *w*^{1118} control larvae, larvae expressing dominant
638 negative Dome$^{\Delta CYT}$ or knocking down *dome*, *hop*, *Stat92E, upd, upd2* and *upd3* under control of
639 *phm-GAL4*, and null *upd3*$^{\Delta 11639}$ mutant larvae. Each dot plots PG size measured as the area
640 occupied by the PG in images of ring glands like those in panels E-H. Horizontal lines represent
641 mean values. Conducted tests were Mann-Whitney tests, except for comparison of both controls
642 and for *phm>dome*$^{\Delta CYT}$, *phm> dome*^{i} and *phm>upd*$^{i-1}$ (two-tailed t-tests). Significance of
643 differences in statistical tests is reported in all figures as follows: $p<0.0001$ (****), $p<0.001$ (***),
644 $p<0.01$ (**), $p<0.05$ (*), and $p>0.05$ (n.s., not significant).

645 (J) Pupation time in *phm-GAL4* and *w*^{1118} controls, and in the indicated JAK/STAT loss of function
646 conditions. Dot-connecting lines plot the accumulated percentage of pupated larvae through time.
647 Time of pupation was computed as hours after L1 ecdysis (see Materials and methods). Number
648 of animals examined is reported in the graph.

Figure 2. JAK/STAT hyperactivation causes PG hypertrophy and delayed metamorphosis

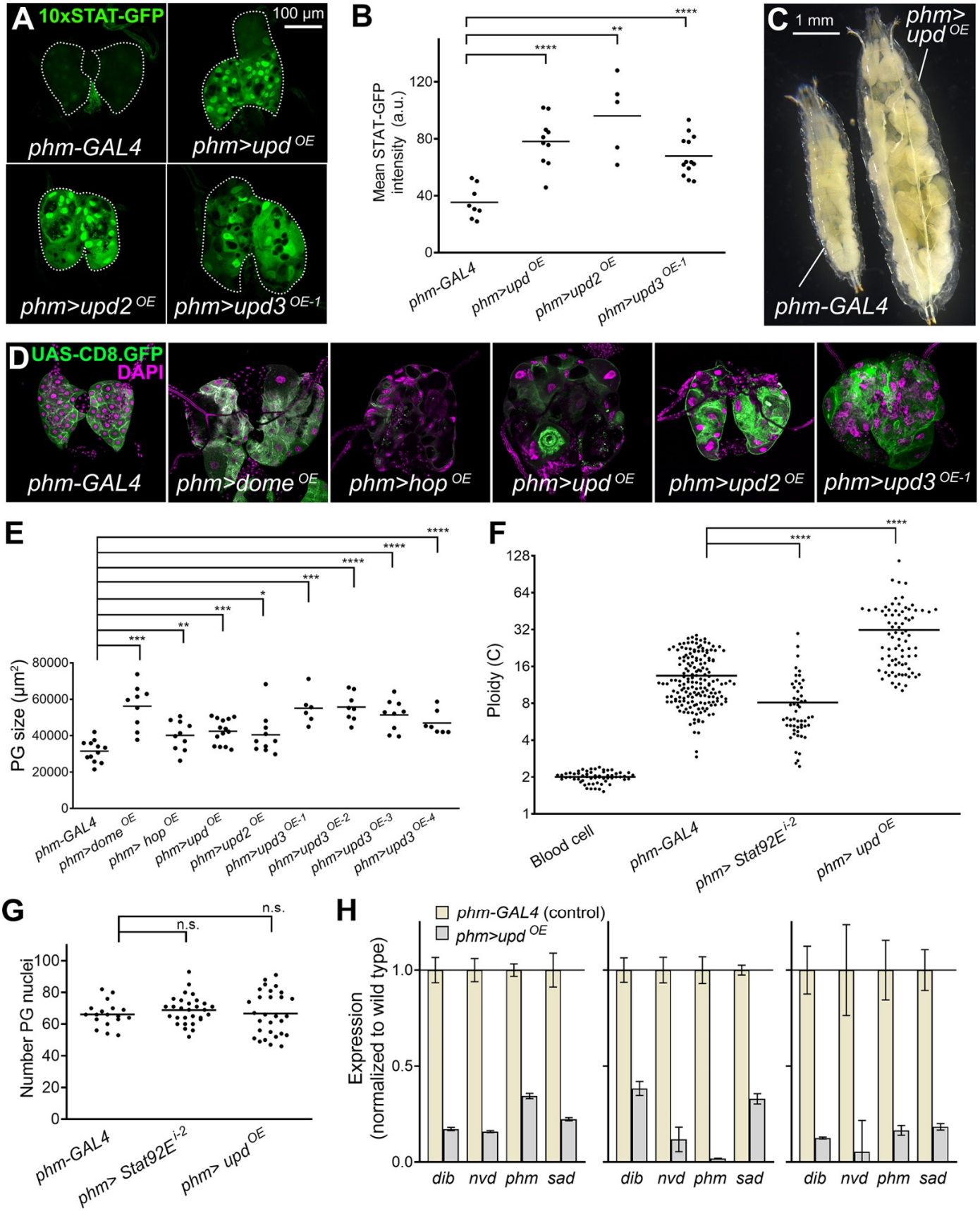

649 **Figure 2. JAK/STAT hyperactivation causes PG hypertrophy and delayed metamorphosis**

650 (A) Expression of JAK/STAT activity reporter 10xSTAT-GFP (green, separate channel in lower
651 subpanels) in the PG of control *phm-GAL4* wL3 larvae and giant larvae overexpressing *upd*, *upd2*,
652 and *upd3* under control of *phm-GAL4*. Dotted lines represent PG outline.

653 (B) Quantification of 10xSTAT-GFP intensity in PG of the larvae overexpressing *upd*, *upd2*, and
654 *upd3* under *phm-GAL4* control. Each dot plots mean GFP intensity (total fluorescence intensity
655 divided by area) in the PG measured in images like those in panel A. Horizontal lines represent
656 mean values. Significance of differences in two-tailed t-tests (*phm>upd*^{OE} and *phm>upd3*^{OE}) and
657 Mann-Whitney tests (*phm>upd2*^{OE}) is reported.

658 (C) Control *phm-GAL4* wL3 larva (left) and larva overexpressing *upd* under *phm-GAL4* control in
659 the PG (*phm>upd*^{OE}, right). Unable to pupate, *phm>upd*^{OE} L3 larvae indefinitely extend their larval
660 period and become giant larvae.

661 (D) Ring glands from a control *phm-GAL4* wL3 larva and from L3 giant larvae overexpressing *dome*,
662 *hop*, *upd*, *upd2* and *upd3* in the PG under control of *phm-GAL4*. *phm-GAL4*-driven CD8.GFP in
663 green. Nuclei stained with DAPI (magenta).

664 (E) Quantification of PG size in wL3 *phm-GAL4* control larvae and in giant larvae overexpressing
665 JAK/STAT pathway components in the PG under control of *phm-GAL4* as indicated. Each dot plots
666 PG size measured from images like those in panel D. Horizontal lines represent mean values.
667 Significance of differences in statistical tests is reported. Conducted tests were two-tailed t-tests
668 (*phm>hop*^{OE}, *phm>upd*^{OE}, *phm>upd3*$^{OE-2}$ and *phm>upd3*$^{OE-3}$), two-tailed t-tests with Welch's
669 correction (*phm>dome*^{OE}) and Mann-Whitney tests (*phm>upd2*^{OE}, *phm>upd3*$^{OE-1}$ and *phm>upd3*$^{OE-}$
670 ^{4}).

671 (F) Quantification of ploidy in PG nuclei of control *phm-GAL4* wL3 larvae, *phm>Stat92E*$^{i\ -2}$ wL3
672 larvae and giant *phm>upd*$^{OE-1}$ larvae. Each dot plots ploidy of a nucleus calculated based on DNA
673 content (DAPI intensity) integrated from confocal stacks of the whole PG and with reference to
674 DNA content in diploid blood cells (see Materials and Methods). n=58, 172, 53 and 80 nuclei,
675 respectively. Horizontal lines represent mean values. Significance of differences in Mann-Whitney
676 tests is reported.

677 (G) Number of nuclei in *phm-GAL4* wL3 larvae, *phm>Stat92E*$^{i\ -2}$ wL3 larvae and giant *phm>upd*^{OE}
678 larvae. Each point represents the number of PG nuclei in one ring gland as counted manually from
679 confocal stacks of the whole PG. n=18, 29 and 29, respectively. Differences were not significant in
680 two-tailed t-tests (*phm>Stat92E*$^{i-2}$) and Mann-Whitney tests (*phm>upd*^{OE}).

681 (H) Quantification of expression of Halloween genes of the ecdysone synthesis pathway by qRT-
682 PCR. Expression levels relative to *rpL23* were normalized to the wild type *phm-GAL4* control. Three
683 biological replicates are shown, each of them with three technical replicates (error bars represent
684 SD).

Figure 3. SUMOylation prevents JAK/STAT hyperactivation during normal PG development

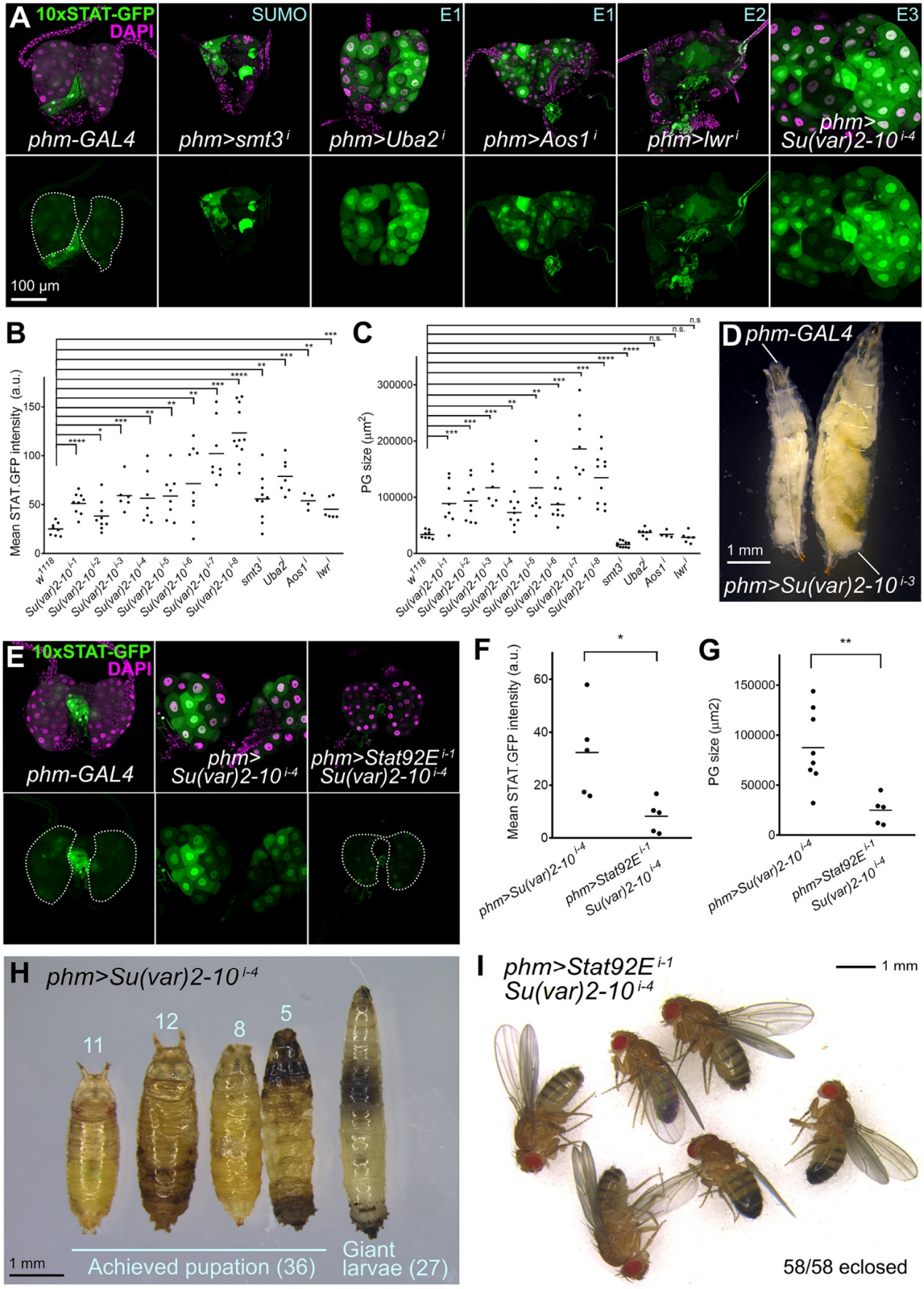

686 **Figure 3. SUMOylation prevents JAK/STAT hyperactivation during normal PG development**

687 (A) Expression of JAK/STAT activity reporter 10xSTAT-GFP (green, separate channel in lower
688 subpanels) in the PG of control *phm-GAL4* wL3 larvae and giant larvae where expression of
689 SUMOylation pathway components has been knocked down under control of *phm-GAL4*. Dotted
690 lines represent PG outline. Nuclei stained with DAPI (magenta).

691 (B) Quantification of 10xSTAT-GFP intensity in PG of control *phm-GAL4* wL3 larvae and giant larvae
692 where expression of SUMOylation pathway components has been knocked down under control
693 of *phm-GAL4*. Each dot plots mean GFP intensity in the PG measured in images like those in panel
694 A. Horizontal lines represent mean values. Significance of differences in statistical tests is reported.
695 Conducted tests were two-tailed t-tests with Welch's correction except for *phm>Su(var)2-10*$^{i-1}$
696 (two-tailed t-test), *phm>Su(var)2-10*$^{i-3}$, *phm>su(var)2-10*$^{i-4}$, *phm>Uba2*^{i}, *phm>Aos1*^{i} and *phm>lwr*^{i},
697 (Mann-Whitney tests).

698 (C) Quantification of PG size in control *phm-GAL4* wL3 larvae and giant larvae where expression
699 of SUMOylation pathway components has been knocked down under control of *phm-GAL4*. Each
700 dot plots PG size measured from images like those in panel A. Horizontal lines represent mean
701 values. Significance of differences in statistical tests is reported. Conducted tests were two-tailed
702 t-tests with Welch's correction except for *phm>smt3*^{i} (two-tailed t-test), and *phm>Su(var)2-10*$^{i-3}$,
703 *phm>Uba2*^{i}, *phm>Aos1*^{i} and *phm>lwr*^{i} (Mann-Whitney tests).

704 (D) Control *phm-GAL4* wL3 larva (left) and giant *phm>Su(var)2-10*$^{i-3}$ larva (right).

705 (E) Expression of JAK/STAT activity reporter 10xSTAT-GFP (green, separate channel in lower
706 subpanels) in the PG of control *phm-GAL4* wL3 larvae (left) and larvae where expression of
707 *Su(var)2-10* (center) and both *Su(var)2-10* and *Stat92E* (right) has been knocked down under
708 control of *phm-GAL4*. Dotted lines represent PG outline. Nuclei stained with DAPI (magenta).

709 (F) Quantification of 10xSTAT-GFP intensity in PG of wL3 larvae where expression of *Su(var)2-10*
710 and both *Su(var)2-10* and *Stat92E* have been knocked down under control of *phm-GAL4*. Each dot
711 plots PG size measured from images like those in panel E. Horizontal lines represent mean values.
712 Difference was significant in a Mann-Whitney test.

713 (G) Quantification of PG size in wL3 larvae where expression of *Su(var)2-10* and both *Su(var)2-10*
714 and *Stat92E* have been knocked down under control of *phm-GAL4*. Each dot plots mean GFP
715 intensity in the PG measured in images like those in panel E. Horizontal lines represent mean
716 values. Difference was significant in a Mann-Whitney test.

717 (H) Defective pupation in *phm>Su(var)2-10*$^{i-4}$ larvae. Number of animals unable to pupate (giant
718 larvae) and exhibiting pupation defects is indicated. Even if pupation was achieved, adults did not
719 eclose.

720 (I) *phm>Su(var)2-10*$^{i-4}$ where *Stat92E* is additionally knocked down reach adulthood.

Figure 4. Extrinsically-produced Upd cytokines can activate JAK/STAT signaling in the PG

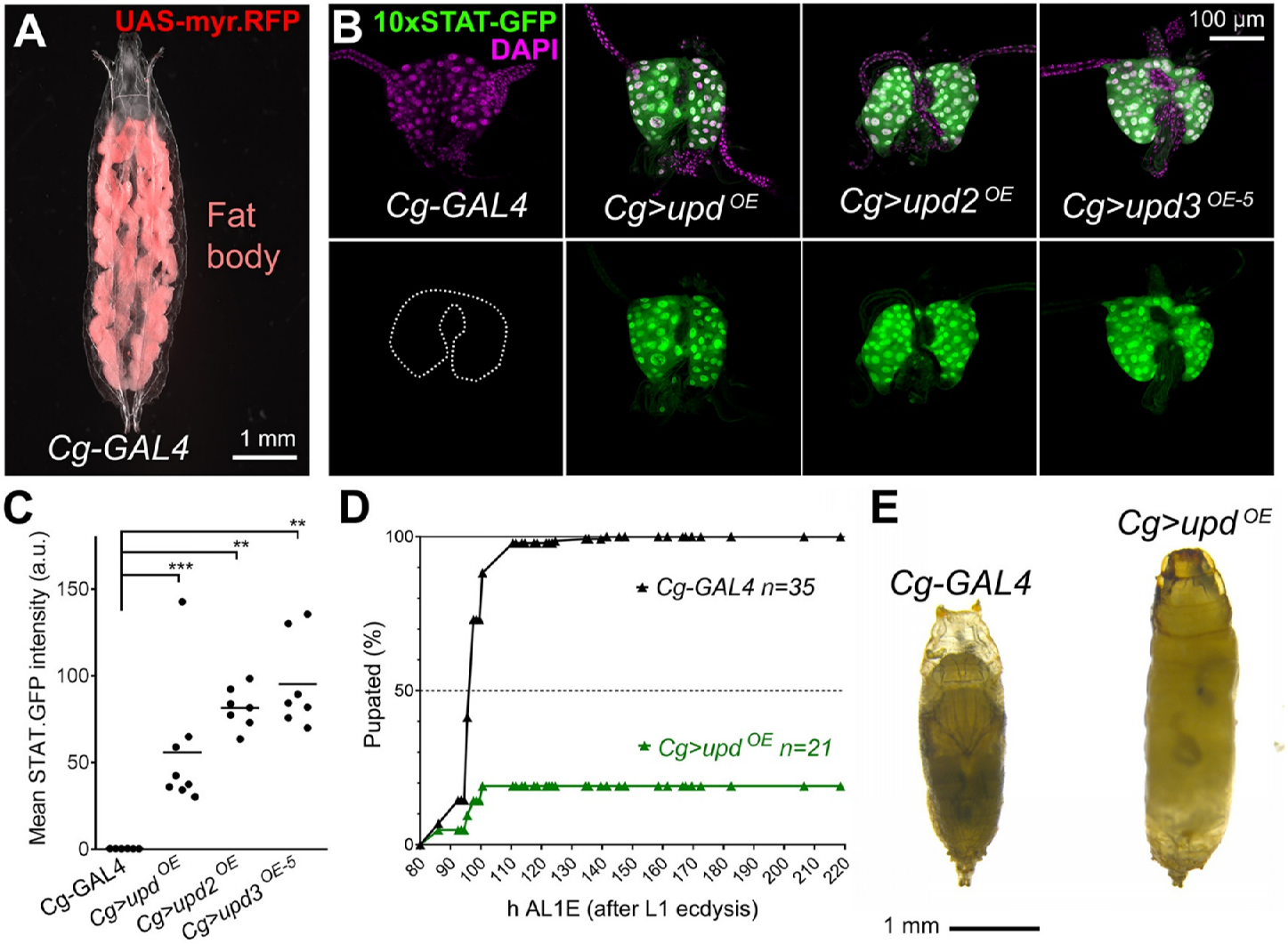

721 **Figure 4. Extrinsically-produced Upd cytokines can activate JAK/STAT signaling in the PG**

722 (A) wL3 larva showing myr.RFP expression in the fat body (red) driven by *Cg-GAL4*. White light and
723 red fluorescence images have been superimposed.

724 (B) Expression of JAK/STAT activity reporter 10xSTAT-GFP (green, separate channel in lower
725 subpanels) in the PG of control *Cg-GAL4* wL3 larvae and giant larvae overexpressing *upd*, *upd2*
726 and *upd3* in the fat body under control of Cg-GAL4. Dotted lines represent PG outline. Nuclei
727 stained with DAPI (magenta).

728 (C) Quantification of 10xSTAT-GFP intensity in PG of control *Cg-GAL4* wL3 larvae and giant larvae
729 overexpressing *upd*, *upd2* and *upd3* in the fat body under control of Cg-GAL4. Each dot plots mean
730 GFP intensity in the PG measured in images like those in panel B. Horizontal lines represent mean
731 values. Significance of differences in Mann-Whitney tests is reported.

732 (D) Pupation time in *Cg-GAL4* control and *Cg>upd*^{OE} animals. Dot-connecting lines plot the
733 accumulated percentage of pupated larvae through time.

734 (E) Control *Cg-GAL4* pupa (left) and pupa of an animal overexpressing *upd* under control of *Cg-*
735 *GAL4* in the fat body (right). Even if pupation is achieved, no adults eclose from *Cg>upd*^{OE} pupae.

Figure 5. Tumors and tissue damage activate PG-extrinsic JAK/STAT signaling to delay metamorphosis

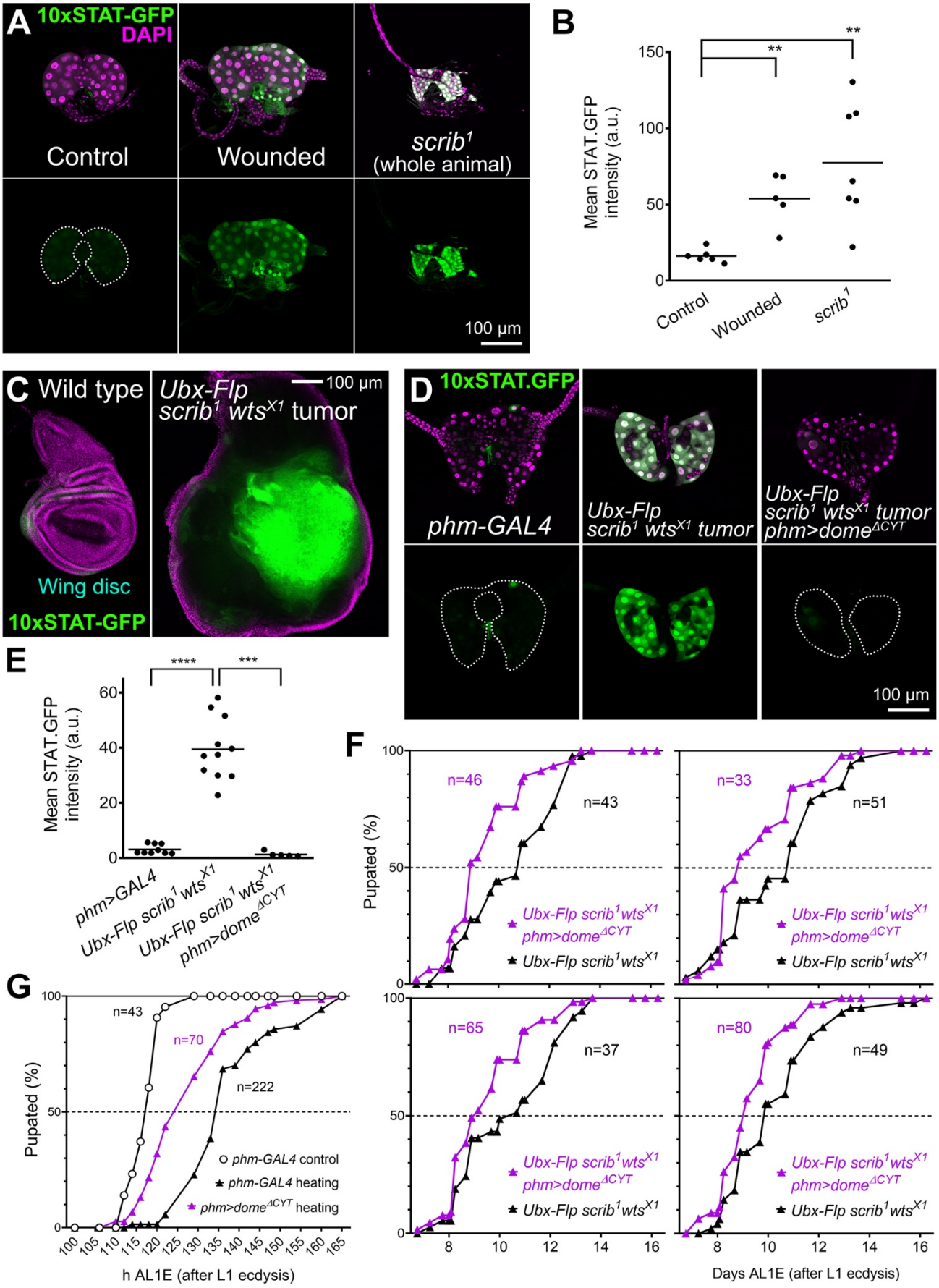

736 **Figure 5. Tumors and tissue damage activate PG-extrinsic JAK/STAT signaling to delay**
737 **metamorphosis**

738 (A) Expression of JAK/STAT activity reporter 10xSTAT-GFP (two copies, green, separate channel in
739 lower subpanels) in the PG of control (left) and puncture-wounded wL3 larvae (center), and of
740 tumor-containing *scrib*^{1} giant larvae. Dotted lines represent PG outline. Nuclei stained with DAPI
741 (magenta).

742 (B) Quantification of 10xSTAT-GFP intensity in PG of control and puncture-wounded wL3 larvae
743 (center), and of tumor-containing *scrib*^{1} giant larvae. Each dot plots mean GFP intensity in the PG
744 measured in images like those in panel A. Horizontal lines represent mean values. Differences in
745 Mann-Whitney tests were significant.

746 (C) Expression of JAK/STAT activity reporter 10xSTAT-GFP (green, separate channel in lower
747 subpanels) in a control wL3 wing imaginal disc (left) and in a wing disc from a wL3 larva containing
748 *scrib*^{1} *wts*^{X1} tumor clones induced through Ubx-Flp-driven mitotic recombination (right). Nuclei
749 stained with DAPI (magenta).

750 (D) Expression of JAK/STAT activity reporter 10xSTAT-GFP (green, separate channel in lower
751 subpanels) in the wL3 PG of control *phm-GAL4* larvae (left), larvae with *scrib*^{1} *wts*^{X1} tumor clones
752 in the wing disc (center) and larvae with *scrib*^{1} *wts*^{X1} wing tumors additionally expressing Dome$^{\Delta CYT}$
753 in the PG under *phm-GAL4* control (right). Dotted lines represent PG outline. Nuclei stained with
754 DAPI (magenta).

755 (E) Quantification of 10xSTAT-GFP intensity in the wL3 PG of control *phm-GAL4* larvae, larvae with
756 *scrib*^{1} *wts*^{X1} wing tumors and larvae with *scrib*^{1} *wts*^{X1} tumors additionally expressing Dome$^{\Delta CYT}$ in
757 the PG under *phm-GAL4* control. Each dot plots mean GFP intensity in the PG measured in images
758 like those in panel D. Horizontal lines represent mean values. Significance of differences in
759 statistical tests is reported. Conducted tests were two-tailed t-test with Welch's correction
760 (control vs. *scrib*^{1} *wts*^{X1} tumor) and Mann-Whitney test (*scrib*^{1} *wts*^{X1} tumor vs. *scrib*^{1} *wts*^{X1} tumor
761 expressing Dome$^{\Delta CYT}$ in the PG).

762 (F) Pupation time in larvae with *scrib*^{1} *wts*^{X1} wing tumors and larvae with *scrib*^{1} *wts*^{X1} tumors
763 additionally expressing Dome$^{\Delta CYT}$ in the PG under *phm-GAL4* control. Four repeats of the
764 experiment are shown. Dot-connecting lines plot the accumulated percentage of pupated larvae
765 through time.

766 (G) Pupation time in *phm-GAL4* control animals and in both *phm-GAL4* and *phm>dome*$^{\Delta CYT}$ animals
767 heated at 39^{0}C for 2.5 hours during the mid L3 stage. Dot-connecting lines plot accumulated
768 percentage of pupated larvae through time.

Figure 6. JAK/STAT target Apontic induces PG hypertrophy, autophagy and metamorphosis delay

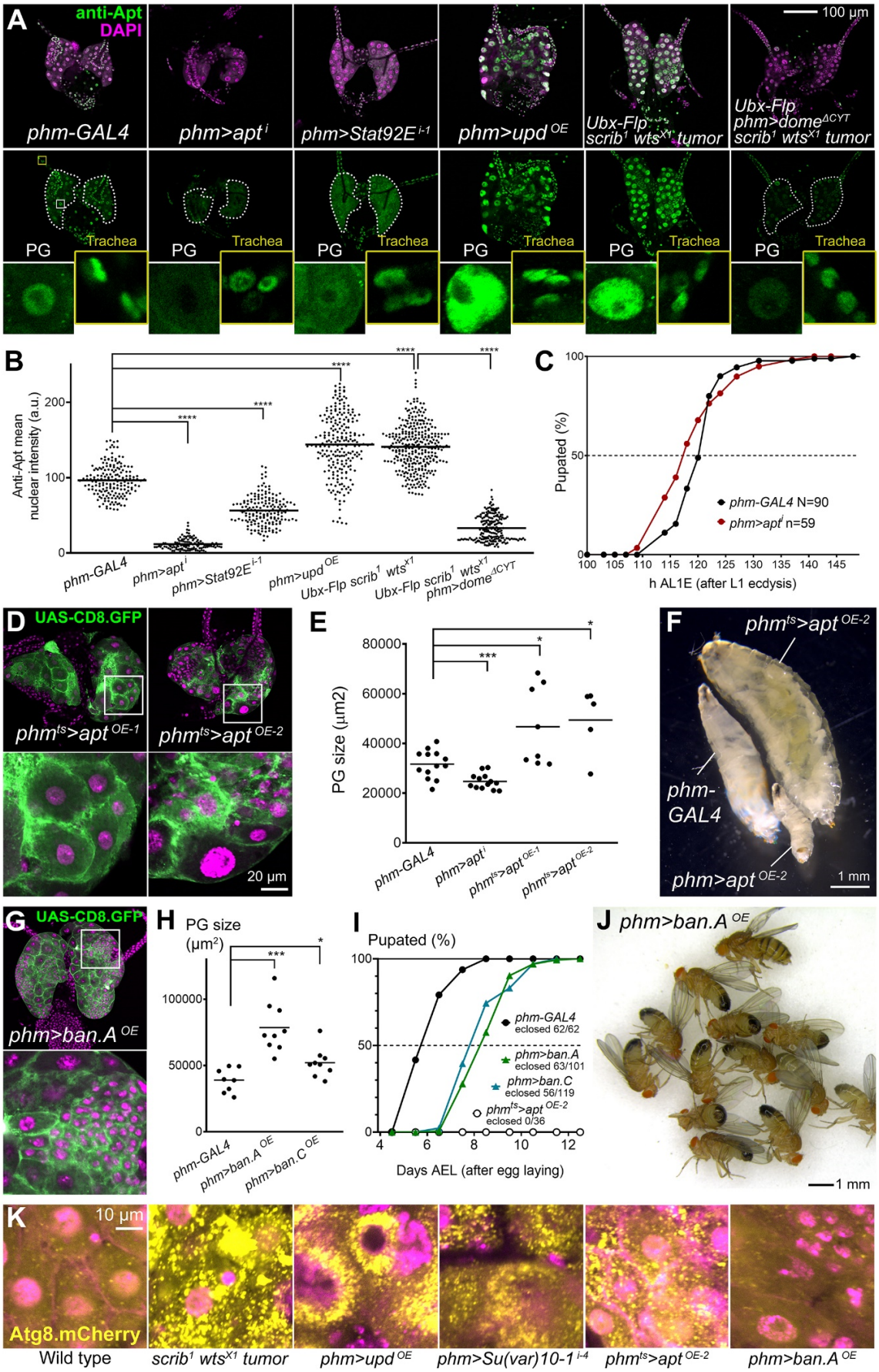

769 **Figure 6. JAK/STAT target Apontic causes PG hypertrophy, autophagy and metamorphosis delay**

770 (A) Anti-Apt antibody stainings (green, separate channel in lower panels) of wL3 ring glands of the
771 indicated genotypes. Dotted lines represent PG outline. Nuclei stained with DAPI (magenta).
772 Higher magnification insets show Apt expression in PG nuclei and in tracheal nuclei as an internal
773 control where levels do not change.

774 (B) Quantification of anti-Apt signal in wL3 PG from larvae of the indicated genotypes. Each dot
775 plots mean GFP intensity in a PG nucleus measured in images like those in panel A. Horizontal
776 lines represent mean values. n=178, 122, 173, 226, 320 and 202 nuclei, respectively. Significance
777 of differences in statistical tests is reported. Conducted tests were Mann-Whitney tests except
778 for *phm-GAL4* control vs. *phm>upd*^{OE} and *scrib*^{1} *wts*^{X1} tumors (two-tailed t-tests with Welch's
779 correction).

780 (C) Pupation time in *phm-GAL4* control and *phm>apt*^{i} animals. Dot-connecting lines plot
781 accumulated percentage of pupated larvae through time.

782 (D) Ring glands from L3 giant larvae overexpressing *apt* in the PG under control of *phm-GAL4* and
783 *tub-GAL80*^{ts}. *phm-GAL4*-driven CD8.GFP in green. Animals were transferred at L2 stage from 18°C
784 to 30^{0}C to initiate *apt* overexpression. Overexpression of *apt* in *phm*^{ts}*>apt*$^{OE-1}$ and *phm*^{ts}*>apt*$^{OE-2}$
785 employs different transgenes (see Table S1). Nuclei stained with DAPI (magenta). Higher
786 magnification insets (white squares) are shown in lower panels.

787 (E) Quantification of PG size in control *phm-GAL4* wL3 larvae, *phm>apt*^{i} wL3 larvae and giant
788 *phm*^{ts}*>apt*^{OE} larvae. Each dot plots PG size measured in images like those in panels A and D.
789 Horizontal lines represent mean values. Significance of differences in statistical tests is reported.
790 Conducted tests were two-tailed t-test (*phm>apt*^{i}), two-tailed t-test with Welch's correction
791 (*phm*^{ts}*>apt*$^{OE-1}$) and Mann-Whitney test (*phm*^{ts}*>apt*$^{OE-2}$).

792 (F) Control *phm-GAL4* wL3 larva, *phm>apt*$^{OE-2}$ L2 larva and giant *phm*^{ts}*>apt*$^{OE-2}$ L3 larva (L2
793 temperature shift).

794 (G) Ring gland from a wL3 larva overexpressing miRNA *bantam* (*ban*) in the PG under *phm-GAL4*
795 control. *phm-GAL4*-driven CD8.GFP in green. Nuclei stained with DAPI (magenta). Higher
796 magnification inset (white squares) in lower panel.

797 (H) Quantification of PG size in control *phm-GAL4* wL3 larvae and larvae overexpressing *ban* under
798 *phm-GAL4* control. Each dot plots PG size measured from images like those in panel G. Horizontal
799 lines represent mean values. Significance of two-tailed t-tests with Welch's correction are
800 reported.

801 (I) Pupation time in *phm-GAL4* control, *phm>ban*^{OE} and *phm*^{ts}*>apt*^{OE} animals. Dot-connecting lines
802 plot the accumulated percentage of pupated larvae through time.

803 (J) Despite metamorphosis delay, *phm>ban*^{OE} animals reach adulthood, unlike *phm*^{ts}*>apt*^{OE}
804 animals.

805 (K) Autophagy marker Atg8.mCherry (yellow) in the PG of wL3 larvae from the indicated
806 genotypes. Nuclei stained with DAPI (magenta).

Figure 7. Intrinsic and extrinsic regulation of PG growth and developmental timing by JAK/STAT

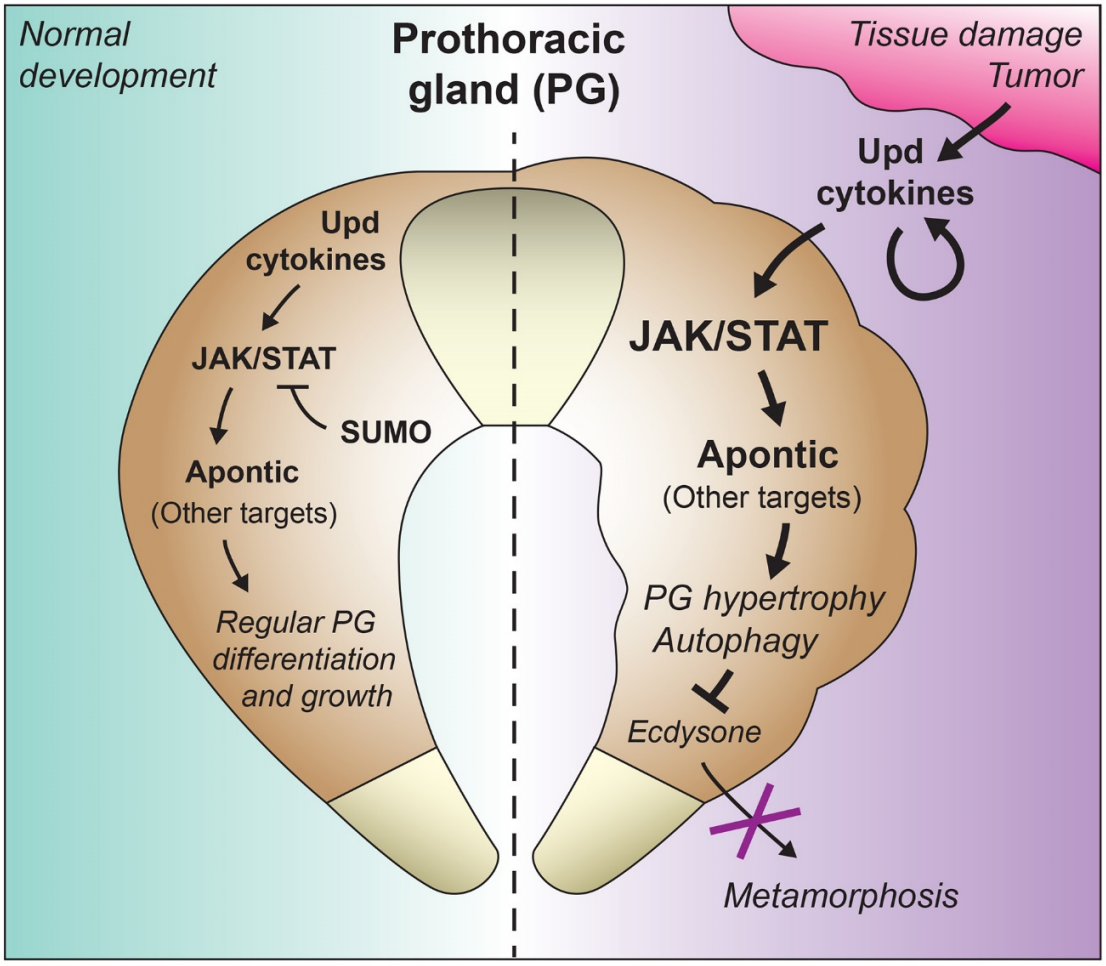

807 **Figure 7. Intrinsic and extrinsic regulation of PG growth and developmental timing by JAK/STAT**

808 Schematic model of the function of JAK/STAT signaling in the PG. Intrinsic expression of Upd3 in
809 the PG activates basal levels of JAK/STAT activity in an autocrine way. Basal JAK/STAT activity is
810 required for correct development of the PG, its loss reducing PG size and slightly advancing the
811 onset of metamorphosis (larva/pupa transition). Levels of JAK/STAT activity are controlled
812 through SUMOylation, involving SUMO E3 ligase Su(var)2-10 (PIAS), thus preventing excessive
813 pathway activation. In conditions producing tumors and tissue damage, Upd cytokines secreted
814 from the damaged tissues and amplified by other tissues (Pastor-Pareja et al., 2008) activate
815 JAK/STAT signaling in the PG, which increases expression of JAK/STAT target Apontic and
816 contributes to strong autophagy induction and inhibition of metamorphosis.

817 **SUPPLEMENTAL MATERIALS**

818

819 **Table S1. Detailed genotypes**

820 Genotypes of animals in all experiments, listed by figure.

821

822 **Table S2. Original strains**

823 Strains used in the study and their origin.